Inorg. Chem. **2004**, *43*, 6954–6964

Reaction Products of $W(CO)_6$ with Formamidines; Electronic Structure of a $W_2(\mu\text{-}CO)_2$ Core with Unsymmetric Bridging Carbonyls

F. Albert Cotton,*,† James P. Donahue,†,§ Michael B. Hall,‡ Carlos A. Murillo,*,† and Dino Villagrán†

Laboratory for Molecular Structure and Bonding and Laboratory for Molecular Simulation, Department of Chemistry, P.O. Box 30012, Texas A&M University, College Station, Texas 77842-3012

Received July 6, 2004

Reactions of $W(CO)_6$ with formamidines contrast with those of $Mo(CO)_6$ and $Cr(CO)_6$ in that the former do not yield quadruply bonded dimetal species. From the reaction of $W(CO)_6$ with HDAniF (HDAniF = *N*,*N*′-di-*p*-anisylformamidine), several new ditungsten carbonyl compounds ($W_2(\mu\text{-}CO)_2(\mu\text{-}DAniF)_2(\eta^2\text{-}DAniF)_2$ (**1**), $W_2(\mu\text{-}CO)_2(\mu\text{-}DAniF)_2(\eta^2\text{-}DAniF)(\eta^2\text{-}CH_2DAniF)$ (**2**), and $W_2(\mu\text{-}CO)(\mu\text{-}CNC_6H_4OCH_3)(\mu\text{-}DAniF)_2(\eta^2\text{-}DAniF)_2$ (**3**)) have been isolated and fully characterized. In **2**, CH_2DAniF represents a DAniF ligand in which a methylene group has been added to one of the nitrogen atoms. This ligand binds to the tungsten atom using a nitrogen and a carbon atom. Compound **1** has a tungsten–tungsten bond distance of 2.476(1) Å and a planar $W_2(\mu\text{-}CO)_2$ core structure which has C_{2h} symmetry with short and long W–C bond distances (1.99(1) and 2.28(1) Å, respectively). DFT calculations on a model of **1** indicate that (a) the C_{2h} instead of D_{2h} symmetry of the ditungsten core may be attributed to W → CO π^* back-bonding interactions and (b) the bond between the tungsten atoms may be formulated as a double bond. The new tetragonal paddlewheel compound $W_2(DAniF)_4$ (**4**) and the edge-sharing bioctahedron $W_2(\mu\text{-}O)(\mu\text{-}NC_6H_3Cl_2)(\mu\text{-}D^{Cl}PhF)_2(\eta^2\text{-}D^{Cl}PhF)_2$ (**5**) ($D^{Cl}PhF$ = *N*,*N*′-di-(3,5-dichlorophenyl)formamidinate) have also been prepared.

Introduction

While quadruply bonded dimolybdenum(II) compounds, that is, molecules built around a Mo_2^{4+} core, are numerous (over 1200), there are only about 10% that many tungsten analogues. A major reason for this difference is the relative dearth of convenient and general methods to synthesize molecules built around W_2^{n+} (n = 4, 5, 6) cores.[1]

The most general route to nearly all Mo_2^{4+} compounds is the reaction of acetic acid, or sometimes another carboxylic acid, with $Mo(CO)_6$ in a high boiling solvent.[1] This produces $Mo_2(O_2CCH_3)_4$, which is a thermodynamically stable compound that, in the crystalline form, can be exposed for months to the atmosphere without apparent decomposition. Ligand replacement reactions on $Mo_2(O_2CCH_3)_4$ lead conveniently to compounds with an extraordinary range of other ligands. No such synthetic entry to W_2^{4+} compounds exists. Reaction of $W(CO)_6$ with acetic acid leads only to $W_3(\mu^3\text{-}O)_2(\mu^2\text{-}O_2CCH_3)_6$ or related species.[2]

The most general route to W_2^{4+} compounds, and the only one to $W_2(O_2CR)_4$ compounds in particular, has been a lengthy, cumbrous, and low yield sequence[3] that begins with the reaction between carefully prepurified WCl_6 and $W(CO)_6$ to give WCl_4. The WCl_4 is then reduced to afford a solution of divalent tungsten, most likely in the form of $W_2Cl_8^{4-}$; the latter has been isolated[4] but is unstable at room temperature. By addition of a carboxylate ligand, RCO_2^-, to a cooled solution of $W_2Cl_8^{4-}$, the desired $W_2(O_2CR)_4$ compound may be obtained. All $W_2(O_2CR)_4$ compounds are much more reactive to oxygen than their molybdenum analogues.

The above synthetic route is also applicable to some other

* To whom correspondence should be addressed. E-mail: cotton@tamu.edu (F.A.C.); murillo@tamu.edu (C.A.M.).

† Laboratory for Molecular Structure and Bonding.

§ Currently at the Department of Chemistry, Tulane University, 6400 Freret Street, New Orleans, LA 70118.

‡ Laboratory for Molecular Simulation.

(2) Cotton, F. A.; Walton, R. A. *Multiple between Metal Atoms*; Oxford University Press: New York, 1993.

(3) Bino, A.; Cotton, F. A.; Dori, Z.; Koch, S.; Küppers, H.; Millar, M.; Sekutowski, J. C. *Inorg. Chem.* **1978**, *17*, 3245.

(4) (a) Sattelberger. A. P.; McLauglin, K. W.; Huffman, J. C. *J. Am. Chem. Soc.* **1981**, *103*, 2280. (b) Santure, D. J.; Sattelberger, A. P. *Inorg. Synth.* **1999**, *26*, 219.

(5) Cotton, F. A.; Mott, G. N.; Schrock, R. R.; Sturgeoff, L. G. *J. Am. Chem. Soc.* **1982**, *104*, 6781.

10.1021/ic049116c CCC: $27.50
Published on Web 09/29/2004

Scheme 1

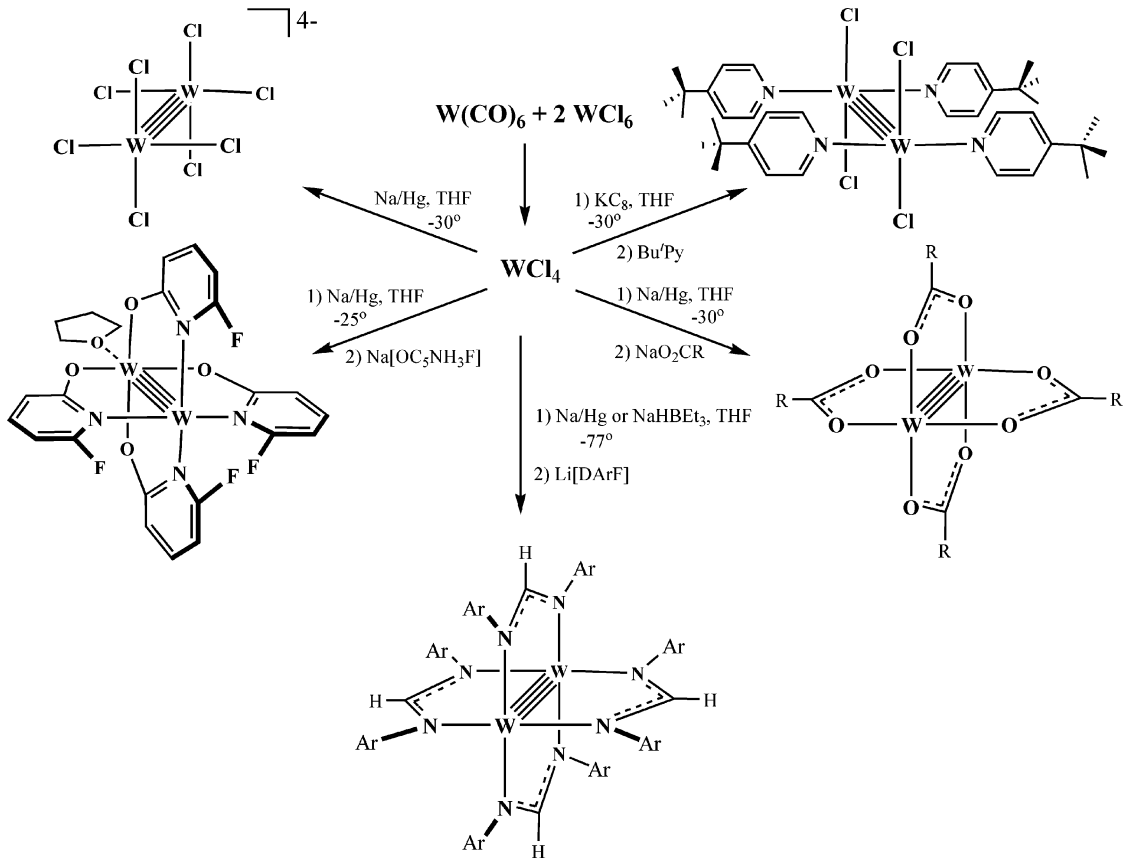

W_2^{4+} compounds as shown in Scheme 1. In addition, the $W_2X_4(PR_3)_4$, W_2X_4(diphos)$_2$, and W_2X_4(py)$_4$ compounds may be obtained fairly conveniently.[5] However, the use of $W(CO)_6$, by far the most convenient starting material, has not been generally practical, although it has been used in a few special instances.[6] Only one unsuccessful attempt to employ $W(CO)_6$ to prepare a $W_2(DArF)_4$ compound has been reported.[7]

Recently, we have been interested in $W_2(hpp)_4$ (hpp = the anion of 1,3,4,6,7,8-hexahydro-2*H*-pyrimido[1,2-*a*]-pyrimidine), as this is the most easily ionized chemical species known,[8] and the ligand hpp structurally resembles the formamidinate groups. We have also been interested in finding routes to mixed ligand complexes of the type $Mo_2(DArF)_n(O_2CCH_3)_{4-n}$, $n = 0-4$, which may be useful synthons for supramolecular chemistry. Because of this, we have undertaken a study of the use of $W(CO)_6$ in reactions with formamidines. It has been found that all of the carbonyl groups in $W(CO)_6$ cannot be immediately expelled (as occurs generally for $Mo(CO)_6$) but instead dinuclear products in which some carbonyls remain are obtained. We report here the characterization of several of these products, whose numerical designations are given in Chart 1.

Chart 1. Numerical Designations for Compounds

$W_2(\mu\text{-}CO)_2(\mu\text{-}DAniF)_2(\eta^2\text{-}DAniF)_2$	**1**
$W_2(\mu\text{-}CO)_2(\mu\text{-}DAniF)_2(\eta^2\text{-}DAniF)(\eta^2\text{-}CH_2DAniF)$	**2**
$W_2(\mu\text{-}CO)(\mu\text{-}CNC_6H_4OCH_3)(\mu\text{-}DAniF)_2(\eta^2\text{-}DAniF)_2$	**3**
$W_2(DAniF)_4$	**4**
$W_2(\mu\text{-}O)(\mu\text{-}NC_6H_3Cl_2)(\mu\text{-}D^{Cl}PhF)_2(\eta^2\text{-}D^{Cl}PhF)_2$	**5**

Experimental Section

Materials and Methods. All manipulations and procedures were conducted under N_2 using either a N_2 drybox or standard Schlenk line techniques. Solvents such as THF, Et_2O, toluene, and hexanes were either distilled from Na/K-benzophenone or were dried and degassed with a Glass Contour solvent purification system. Chlorobenzene and *o*-dichlorobenzene were dried over freshly activated molecular sieves and degassed with vigorous N_2 bubbling immediately prior to use, and CH_2Cl_2 was dried and distilled from P_2O_5. The compounds WCl_4,[3b] HDAniF[9] (HDAniF = *N*,*N*′-di-*p*-anisylformamidine, Scheme 2), and $HD^{Cl}PhF$[9] ($HD^{Cl}PhF$ = *N*,*N*′-

(5) (a) Cotton, F. A.; Felthouse, T. R.; Lay, D. G. *J. Am. Chem. Soc.* **1980**, *102*, 1431. (b) Cotton, F. A.; Felthouse, T. R. *Inorg. Chem.* **1981**, *20*, 3880. (c) Schrock, R. R.; Sturgeoff, L. G.; Sharp, P. R. *Inorg. Chem.* **1983**, *22*, 2801. (d) Canich, J. A. M.; Cotton, F. A. *Inorg. Chim. Acta* **1988**, *142*, 69. (e) Fryzuk, M. D.; Kreiter, C. G.; Sheldrick, W. S. *Chem. Ber.* **1989**, *122*, 851. (f) Cotton, F. A.; Eglin, J. L. *Inorg. Chem.* **1993**, *32*, 681. (g) Cotton, F. A.; Dikarev, E. V.; Gu, J.; Herrero, S.; Modec, B. *Inorg. Chem.* **2000**, *39*, 5407.

(6) (a) Cotton, F. A.; Fanwick, P. E.; Niswander, R. H.; Sekutowski, J. C. *J. Am. Chem. Soc.* **1978**, *100*, 4725. (b) Cotton, F. A.; Ilsley, W. H.; Kaim, W. *Inorg. Chem.* **1980**, *19*, 1453. (c) Cotton, F. A.; Niswander, R. H.; Sekutowski, J. C. *Inorg. Chem.* **1979**, *18*, 1152. (d) Kim, J. C.; Goedken, V. L.; Lee, B. M. *Polyhedron* **1996**, *15*, 57.

(7) de Roode, W. H.; Vrieze, K.; Koerner von Gustorf, E. A.; Ritter, A. *J. Organomet. Chem.* **1977**, *135*, 183.

(8) Cotton, F. A.; Gruhn, N. E.; Gu, J.; Huang, P.; Lichtenberger, D. L.; Murillo, C. A.; Van Dorn, L. O.; Wilkinson, C. C. *Science* **2002**, *298*, 1971.

(9) Lin, C.; Protasiewicz, J. D.; Smith, E. T.; Ren, T. *Inorg. Chem.* **1996**, *35*, 6422.

Scheme 2. Structure of the Molecule from Which the DAniF Ligand Is Derived

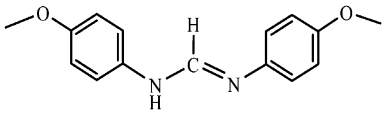

HDAniF = *N*,*N*′-di-*p*-anisylformamidine

di-(3,5-dichlorophenyl)formamidine) were prepared by literature methods, while $W(CO)_6$ was purchased from a commercial source.

Physical Methods. Elemental analyses were performed by Canadian Microanalytical Service, Delta, British Columbia, upon crystalline samples that were redissolved in CH_2Cl_2 and dried overnight under vacuum. ^{1}H NMR spectra were recorded on a Varian XL-200AA spectrometer with chemical shifts referenced to the protonated solvent residual. Absorption spectra were measured at room temperature under N_2 using a Shimadzu UV-2501 PC spectrophotometer. The cyclic voltammograms were taken with a CH Instruments model-CHI620A electrochemical analyzer in 0.1 M Bu_4NPF_6 solution in CH_2Cl_2 with Pt working and auxiliary electrodes, a Ag/AgCl reference electrode, and a scan rate of 100 mV/s. All the potential values are referenced to the Ag/AgCl electrode, and under the present experimental conditions, the $E_{1/2}$ for the Fc^+/Fc couple consistently occurred at +440 mV.

X-ray Structure Determinations. Needle-shaped crystals of **1**·CH_2Cl_2 (red) and block-shaped crystals of **4** (red) were grown over a period of several days by layering CH_2Cl_2 solutions (5−10 mL) with several volume equivalents of hexanes (40−50 mL). Red, plate-shaped crystals of **2** formed after layering a chlorobenzene solution with a 1:15 Et_2O/hexanes mixture. Brown-black needles of **3**·C_6H_{14} were prepared by diffusing the vapor of mixed hexanes into a chlorobenzene solution. Small amounts of fine, green plate crystals of **5** slowly deposited over a 10−14 day period from a toluene solution of $W_2(D^{Cl}PhF)_4$ that had been briefly exposed to air and then layered with hexanes.

All crystals were coated with Paratone oil and mounted on a quartz fiber or a nylon cryoloop affixed to a goniometer head. All diffraction data were collected using a Bruker SMART 1000 CCD area detector system using ω scans of 0.3 deg/frame with 30, 60, or 90 s frames such that 1271 frames were collected for a full hemisphere of data. The first 50 frames were re-collected at the end of the data collection to monitor for crystal decay, but no significant decomposition was observed. Cell parameters were determined using the program SMART.[10] Data reduction and integration were performed with the software package SAINT,[11] which corrects for Lorentz and polarization effects, while absorption corrections were applied by using the program SADABS.[11]

Space groups for all compounds structurally characterized by X-ray crystallography were initially determined with the aid of the program XPREP, which is part of the SHELX software package.[12] Compounds **1**, **4**, and **5** yield good solutions and well-behaved refinements in $P\bar{1}$. For **2**, intensity statistics favor a noncentric space group, which is consistent with the asymmetry in this molecule that is introduced by the insertion of the CH_2 group between one pair of tungsten and chelating nitrogen atoms. Compound **2** refines optimally in $P2_1$ as a slight racemic twin (Flack parameter ≈ 0.22). Refinement of **2** in $P2_1/c$ to the fullest extent possible resulted in appreciably higher *R* factors, a poorer goodness-of-fit, and larger residual peaks. A similar situation is found with compound **3** in which the bent μ-$CNC_6H_4OCH_3$ group removes all symmetry from the molecule, and intensity statistics in the reflection data favor a noncentric space group. Compound **3** refines optimally in *Cc* as a racemic twin (Flack parameter ≈ 0.35). Efforts to solve this structure in centrosymmetric *C*2/*c* or in an orthorhombic space group were unsuccessful in producing a workable solution.

In all structures, the positions of the W atoms or other heavy atoms were found via direct methods using the SHELX software.[12] The remaining non-hydrogen atoms were revealed by subsequent cycles of least-squares refinement followed by difference Fourier syntheses. In compound **1**, three of the four anisyl groups in the half-molecule that constitutes the asymmetric unit were disordered and modeled as a distribution between two positional variants. A similar disorder was observed for the μ-$CNC_6H_4OCH_3$ group in **3**, which was also refined as an optimal fit between two different orientations. The interstitial CH_2Cl_2 that crystallizes with **1** was disordered but could be refined satisfactorily as a 1:2 ratio over two positions. A molecule of hexanes cocrystallized with **3** and appeared as a highly disordered set of peaks in the electron density maps. These peaks were refined as carbon atoms with partial site occupancies that collectively amounted to six carbon atoms. For **2** and **3**, only the W atoms were refined anisotropically. In all the structures, hydrogen atoms were added in calculated positions and treated as riding atoms with isotropic displacement parameter values equal to 1.2 times those of the carbon atoms to which they were attached. Cell parameters and refinement results for all compounds are summarized in Table 1 while selected metric parameters are collected in Tables 2−6.

Computational Details. Density functional theory (DFT)[13] calculations were performed with the hybrid Becke-3 parameter exchange functional[14] and the Lee−Yang−Parr nonlocal correlation functional[15] (B3LYP) implemented in the Gaussian 98 (Revision A.9) program suite.[16] Double-ζ quality basis sets (D95)[17] were used on nonmetal atoms (carbon, nitrogen, oxygen, and hydrogen). An effective core potential (ECP) representing the 1s2s2p3s3p3d4s4p4d core was used for the tungsten atoms with a double-ζ basis set (LANL2DZ).[18] The convergence criterion for the self-consistent field cycles on all calculations was increased from the default value to 10^{-8}. The calculations were carried out on simplified models in

(10) *SMART for Windows NT*, Version 5.618; Bruker Analytical X-ray Systems: Madison, WI, 2000.
(11) *SAINT+ for NT*, Version 6.28A; Bruker Analytical X-ray Systems: Madison, WI, 2001.
(12) Sheldrick, G. M. *SHELX-97 Programs for Crystal Structure Analysis*; Institüt für Anorganische Chemie der Universität: Göttingen, Germany, 1998.
(13) (a) Hohenberg, P.; Kohn, W. *Phys. Rev.* **1964**, *136*, B864. (b) Parr, R. G.; Yang, W. *Density-Functional Theory of Atoms and Molecules*; Oxford University Press: Oxford, 1989.
(14) (a) Becke, A. D. *Phys. Rev. A* **1988**, *38*, 3098. (b) Becke, A. D. *J. Chem. Phys.* **1993**, *98*, 1372. (c) Becke, A. D. *J. Chem. Phys.* **1993**, *98*, 5648.
(15) Lee, C.; Yang, W.; Parr, R. G. *Phys. Rev. B* **1988**, *37*, 785.
(16) Frisch, M. J.; Trucks, G. W.; Schlegel, H. B.; Scuseria, G. E.; Robb, M. A.; Cheeseman, J. R.; Zakrzewski, V. G.; Montgomery, J. A., Jr.; Stratmann, R. E.; Burant, J. C.; Dapprich, S.; Millam, J. M.; Daniels, A. D.; Kudin, K. N.; Strain, M. C.; Farkas, O.; Tomasi, J.; Barone, V.; Cossi, M.; Cammi, R.; Mennucci, B.; Pomelli, C.; Adamo, C.; Clifford, S.; Ochterski, J.; Petersson, G. A.; Ayala, P. Y.; Cui, Q.; Morokuma, K.; Malick, D. K.; Rabuck, A. D.; Raghavachari, K.; Foresman, J. B.; Cioslowski, J.; Ortiz, J. V.; Stefanov, B. B.; Liu, G.; Liashenko, A.; Piskorz, P.; Komaromi, I.; Gomperts, R.; Martin, R. L.; Fox, D. J.; Keith, T.; Al-Laham, M. A.; Peng, C. Y.; Nanayakkara, A.; Gonzalez, C.; Challacombe, M.; Gill, P. M. W.; Johnson, B. G.; Chen, W.; Wong, M. W.; Andres, J. L.; Head-Gordon, M.; Replogle, E. S.; Pople, J. A. *Gaussian 98*, revision A.9; Gaussian, Inc.: Pittsburgh, PA, 1998.
(17) Dunning, T. H.; Hay, P. J. In *Modern Theoretical Chemistry. 3. Methods of Electronic Structure Theory*; Schaefer, H. F., III, Ed.; Plenum Press: New York, 1977; pp 1−28.
(18) (a) Wadt, W. R.; Hay, P. J. *J. Chem. Phys.* **1985**, *82*, 284. (b) Hay, P. J.; Wadt, W. R. *J. Chem. Phys.* **1985**, *82*, 299.

Table 1. Crystallographic Data for Tungsten Formamidinate Compounds

	1·CH_2Cl_2	**2**	**3**·C_6H_{14}	**4**	**5**
formula	$C_{63}H_{62}Cl_2N_8O_{10}W_2$	$C_{63}H_{62}N_8O_{10}W_2$	$C_{75}H_{81}N_9O_{10}W_2$	$C_{60}H_{60}N_8O_8W_2$	$C_{58}H_{31}Cl_{18}N_9OW_2$
fw, g·mol^{-1}	1529.81	1458.91	1636.19	1388.86	1875.72
cryst syst	triclinic	monoclinic	monoclinic	triclinic	triclinic
space group	$P\bar{1}$	$P2_1$	Cc	$P\bar{1}$	$P\bar{1}$
a (Å)	12.924(3)	12.657(1)	28.69(1)	10.272(2)	12.708(3)
b (Å)	15.897(4)	13.267(1)	12.844(5)	10.380(2)	13.846(4)
c (Å)	16.704(4)	17.925(2)	18.647(8)	13.952(3)	21.235(6)
α (deg)	69.945(4)	90	90	80.42(3)	72.053(5)
β (deg)	74.968(5)	105.802(2)	90.09(1)	75.61(3)	75.449(4)
γ (deg)	87.891(5)	90	90	81.69(3)	71.703(5)
V (Å^3)	3108(1)	2896.2(4)	6872(5)	1412.5(5)	3325(2)
Z	2	2	4	1	2
d_{calc} (g·cm^{-1})	1.635	1.673	1.582	1.633	1.874
μ (mm^{-1})	3.848	4.036	3.412	4.131	4.229
2θ range, deg	3.3−50.1	3.3−50.0	4.1−45.2	4.7−55.0	3.2−45.1
λ, Å	0.71073	0.71073	0.71073	0.71073	0.71073
T, °C	−60	−60	−60	−60	−60
GOF	1.037	1.040	1.003	1.069	1.041
R1,[a] wR2[b] ($I > 2\sigma(I)$)	0.064, 0.170	0.072, 0.135	0.054, 0.119	0.022, 0.052	0.051, 0.112

[a] $R1 = \sum||F_o| - |F_c||/\sum|F_o|$. [b] $wR2 = [\sum[w(F_o^2 - F_c^2)^2]/\sum w(F_o^2)^2]^{1/2}$, $w = 1/[\sigma^2(F_o^2) + (aP)^2 + bP]$, where $P = [\max(F_o^2 \text{ or } 0) + 2(F_c^2)]/3$.

which each *p*-anisyl substituent was replaced with a hydrogen atom. To gain insight into the electronic transitions responsible for the observed UV−vis spectrum of **1**, time-dependent density functional theory[19] (TD-DFT) calculations were performed using the Gaussian program suite. All calculations were run on an Origin 3800 64-processor SGI computer located at the Texas A&M Supercomputing facility.

Syntheses. Preparation of W$_2$(μ-CO)$_2$(μ-DAniF)$_2$(η^2-DAniF)$_2$ (1), W$_2$(μ-CO)$_2$(μ-DAniF)$_2$(η^2-DAniF)(η^2-CH$_2$DAniF) (2), and W$_2$(μ-CO)(μ-CNC$_6$H$_4$OCH$_3$)(μ-DAniF)$_2$(η^2-DAniF)$_2$ (3). An oven-dried 100 mL Schlenk flask was charged with a stir bar, W(CO)$_6$ (2.75 g, 7.81 mmol), HDAniF (5.00 g, 19.5 mmol), *o*-dichlorobenzene (30 mL), and hexanes (5 mL).[20] The flask was fitted with a water condenser, and the system was cycled under vacuum and filled with N_2 several times. This mixture was heated to 185 °C for 15 h with rapid stirring and then was cooled to ambient temperature. This dark solution was concentrated under vacuum to an oily residue, redissolved in a minimal amount of CH_2Cl_2, and chromatographed on a column packed with SiO_2 (60−200 mesh) using 0.5% THF in CH_2Cl_2 as eluant. The eluant was collected in 10 mL fractions. After the leading bright red band was collected, elution was continued with 5% THF in CH_2Cl_2, which moved an additional brown band from the column which was also collected in fractions. The purity of these individual fractions was assessed by ^{1}H NMR spectroscopy. Those fractions which were still mixed were combined and repeatedly column chromatographed until only one product was observed in the fraction (∼10−12 successive columns).

W$_2$(μ-CO)$_2$(μ-DAniF)$_2$(η^2-DAniF)$_2$ (1). Yield: 0.317 g, 5.6%. $R_f = 0.37$ in 0.5% THF in CH_2Cl_2; $R_f = 0.79$ in 5% THF in CH_2Cl_2. ^{1}H NMR δ (ppm in $CDCl_3$): 9.11 (s, 2H, μ-NC*H*N−; d, J = 7.1 Hz for ^{1}H−^{183}W),[21] 8.30 (s, 2H, η-NC*H*N−), 6.98 (d, 8H, aromatic C−H), 6.70 (d, 8H, aromatic C−H), 6.61 (d, 8H, aromatic C−H), 6.47 (d, 8H, aromatic C−H), 3.77 (s, 12H, −OCH_3), 3.73 (s, 12H, −OCH_3). IR (KBr, cm^{-1}): 1747 (vs, ν_{CO}). Absorption spectrum (CH_2Cl_2) λ_{max} (ϵ_M): 243 (sh, 61000) 292 (55100), 330 (sh, 32600), 420 (sh, 8140), 575 (2370). ESI-MS: m/z 1445 (M$^+$), 1389 (M$^+$ − 2CO). Anal. Calcd for $C_{62}H_{60}N_8O_{10}W_2$: C, 51.54; H, 4.19; N, 7.76. Found: C, 51.39; H, 4.20; N, 7.63.

W$_2$(μ-CO)$_2$(μ-DAniF)$_2$(η^2-DAniF)(η^2-CH$_2$DAniF) (2). Yield: 0.793 g, 13.9%. $R_f = 0.34$ in 0.5% THF in CH_2Cl_2; $R_f = 0.77$ in 5% THF in CH_2Cl_2. ^{1}H NMR δ (ppm in $CDCl_3$): 9.07 (s, 2H, μ-NC*H*N−; d, J = 6.9 Hz for ^{1}H−^{183}W),[21] 8.27 (s, 1H, η-NC*H*N−), 7.35 (s, 1H, η-NC*H*N−), 7.06 (d, 4H, aromatic C−H), 6.99 (d, 4H, aromatic C−H), 6.43−6.78 (m, 24H, aromatic C−H), 3.78 (s, 3H, −OCH_3), 3.773 (s, 3H, −OCH_3), 3.766 (s, 3H, −OCH_3), 3.76 (s, 3H, −OCH_3), 3.74 (s, 6H, −OCH_3), 3.73 (s, 6H, −OCH_3), 3.10 (s, br, 2H, −H_2CW). ^{13}C NMR δ (ppm in $CDCl_3$): 275.72 (μ-CO), 265.29 (μ-CO), 168.19, 165.03, 162.83, 157.65, 157.50, 157.38, 156.77, 155.74, 155.32, 147.43, 147.16, 145.76, 141.59, 141.31, 139.25, 126.98, 126.72, 125.95, 122.84, 122.28, 120.26, 113.93, 113.75, 113.35, 113.12, 112.94, 69.40, 55.61, 55.56, 55.52, 55.44. IR (KBr, cm^{-1}): 1745 (vs, ν_{CO}). Absorption spectrum (CH_2Cl_2) λ_{max} (ϵ_M): 247 (67100), 288 (sh, 49300), 329 (sh, 29100), 365 (sh, 19100), 404 (sh, 9180), 560 (1600). ESI-MS: m/z 1459 (M$^+$), 1403 (M$^+$ − 2CO). Anal. Calcd for $C_{63}H_{62}N_8O_{10}W_2$: C, 51.87; H, 4.28; N, 7.68. Found: C, 51.87; H, 4.23; N, 7.57.

W$_2$(μ-CO)(μ-CNC$_6$H$_4$OCH$_3$)(μ-DAniF)$_2$(η^2-DAniF)$_2$ (3). Yield: 0.051 g, 0.8%. $R_f = 0.32$ in 0.5% THF in CH_2Cl_2. ^{1}H NMR δ (ppm in $CDCl_3$): 9.05 (s, 2H, μ-NC*H*N−; d, J = 8.1 Hz for ^{1}H−^{183}W),[21] 8.37 (s, 2H, η-NC*H*N−), 6.99 (d, 8H, aromatic C−H), 6.51−6.73 (m, 20H, aromatic C−H), 6.33−6.37 (m, 8H, aromatic C−H), 3.77 (s, 6H, −OCH_3), 3.74 (s, 3H, −OCH_3), 3.72 (s, 12H, −OCH_3), 3.66 (s, 6H, −OCH_3). Absorption spectrum (CH_2Cl_2) λ_{max} (ϵ_M): 251 (63900) 287 (62400), 333 (sh, 37500), 443 (sh, 6660). ESI-MS: m/z 1550 (M$^+$). Anal. Calcd for $C_{69}H_{67}N_9O_{10}W_2$: C, 53.47; H, 4.36; N, 8.13. Found: C, 53.13; H, 4.43; N, 7.92.[22]

W$_2$(DAniF)$_4$ (4). This compound was prepared from WCl_4 (1.00 g, 3.07 mmol) by a procedure analogous to that described in the literature for W$_2$(D^{Cl}PhF)$_4$,[23] but with the use of KC_8 as reducing agent rather than NaHBEt$_3$ or Na/Hg amalgam. Yield: 0.84 g, 40%. ^{1}H NMR (ppm in $CDCl_3$): 8.30 (s, 4H, −NC*H*N−), 6.53 (d, 16H,

(19) Casida, M. E.; Jamorski, C.; Casida, K. C.; Salahub, D. R. *J. Chem. Phys.* **1998**, *108*, 4439.

(20) The use of hexanes is essential to prevent unreacted W(CO)$_6$ from subliming into the reflux condenser and forming a potentially dangerous plug through which excess pressure of CO gas cannot be released.

(21) The −NC*H*N− singlet is superimposed over the small doublet resulting from ^{1}H−^{183}W coupling. The coupling constant is relatively small since the ^{1}H nucleus is three bonds removed from the ^{183}W. This doublet is very slightly offset from the singlet, apparently due to a small isotope shift effect. See: Raynes, W. T. Nuclear Shielding. In *Nuclear Magnetic Resonance*; Harris, R. H., Ed.; Alden Press: Oxford, 1972; pp 42−43.

(22) These values represent the average of two different analyses performed upon the same sample.

aromatic C−H, $J = 9.0$ Hz), 6.23 (d, 16H, aromatic C−H, $J = 9.0$ Hz), 3.71 (s, 24H, $-OCH_3$). Absorption spectrum (CH_2Cl_2) λ_{max} (ϵ_M): 277 (63400), 335 (sh, 26600), 371 (sh, 15200), 412 (sh, 10600). Anal. Calcd for $C_{60}H_{60}N_8O_8W_2$: C, 51.89; H, 4.35; N, 8.07. Found: C, 51.64; H, 4.41; N, 8.05.

$W_2(\mu\text{-}O)(\mu\text{-}NC_6H_3Cl_2)(\mu\text{-}D^{Cl}PhF)_2(\eta^2\text{-}D^{Cl}PhF)_2$ (5). A solution of $W_2(D^{Cl}PhF)_4$ (0.030 g, 0.018 mmol) in 10 mL of toluene was layered with 50 mL of hexanes without careful exclusion of air. The Schlenk tube was allowed to stand undisturbed for a period of 10−14 days, during which time the solution slowly turned light green and deposited dark crystals of **5** at the bottom of the tube. After two weeks, the solvent and other loose solids were decanted from the tube, and the dark green crystals collected and recrystallized in the open air by diffusion of hexanes vapor into a concentrated toluene solution. Yield: 0.0133 g, 40%. ^{1}H NMR (ppm in CD_2Cl_2): 8.77 (s, 2H, μ-NC*H*N−; d, $J = 4.9$ Hz for ^{1}H−^{183}W),[21] 8.73 (s, 2H, η-NC*H*N−; d, $J = 4.3$ Hz for ^{1}H−^{183}W),[21] 8.02 (d, 4H, *ortho* C−H, $J = 1.8$ Hz), 7.31 (t, 2H, *para* C−H, $J = 1.8$ Hz), 7.20 (t, 2H, *para* C−H, $J = 1.8$ Hz), 7.15 (t, 4H, *para* C−H, $J = 1.8$ Hz), 6.93 (t, 1H, *para* C−H, $J = 1.8$ Hz), 6.57 (d, 8H, *ortho* C−H, $J = 1.8$ Hz), 6.39 (d, 4H, *ortho* C−H, $J = 1.8$ Hz), 6.25 (d, 2H, *ortho* C−H, $J = 1.8$ Hz). Absorption spectrum (CH_2Cl_2) λ_{max} (ϵ_M): 308 (sh, 46900), 313 (47500), 359 (sh, 18400), 405 (sh, 9470), 653 (5120). Anal. Calcd for $C_{58}H_{31}Cl_{18}N_9OW_2$: C, 37.14; H, 1.67; N, 6.72. Found: C, 37.49; H, 1.69; N, 6.72.

Results and Discussion

Syntheses and Structures. The reaction of HDAniF with $W(CO)_6$ in a mixture of 1:10 hexanes/*o*-dichlorobenzene under reflux for 15 h did not yield any crystalline material upon cooling nor did it yield a precipitate of any sort. This is quite a different result from that obtained with the analogous molybdenum system.[9] However, an analysis of the dark reaction mixture by TLC showed that it contained some red solutes that would be amenable to purification by chromatography using silica. When the crude product mixture was dissolved in a minimal amount of 0.5% THF in CH_2Cl_2 (v/v), passing it through a silica column left the majority of the material at or near the top, but a bright red band was eluted. Collection of the eluant in ∼10 mL fractions, each of which was examined by ^{1}H NMR spectroscopy, revealed the elution in close succession of three distinct compounds which share the common feature of having a $W_2(\mu\text{-}CO)(\mu\text{-}DAniF)_2(\eta^2\text{-}DAniF)$ moiety. In order of elution, these compounds are $W_2(\mu\text{-}CO)_2(\mu\text{-}DAniF)_2(\eta^2\text{-}DAniF)_2$ (**1**), $W_2(\mu\text{-}CO)_2(\mu\text{-}DAniF)_2(\eta^2\text{-}DAniF)(\eta^2\text{-}CH_2DAniF)$ (**2**), and $W_2(\mu\text{-}CO)(\mu\text{-}CNC_6H_4OCH_3)(\mu\text{-}DAniF)_2(\eta^2\text{-}DAniF)_2$ (**3**). All three compounds are relatively air stable and may be handled briefly in the laboratory atmosphere both as solids and in solution without appreciable decomposition. Each compound was obtained in crystalline form as described in the Experimental Section.

The structure of **1** is shown in Figure 1 along with a list of relevant bond lengths and angles (Table 2). This molecule resides on an inversion center in the space group $P\bar{1}$ and has a W−W bond length of 2.476(1) Å that is clearly indicative of some degree of metal−metal bonding. An important feature in this structure is the highly unsymmetrical nature of the bridging CO ligands, which lowers the molecular symmetry from D_{2h} to C_{2h}. The difference of 0.29(2) Å between the W−C and W−C(1A) bond lengths

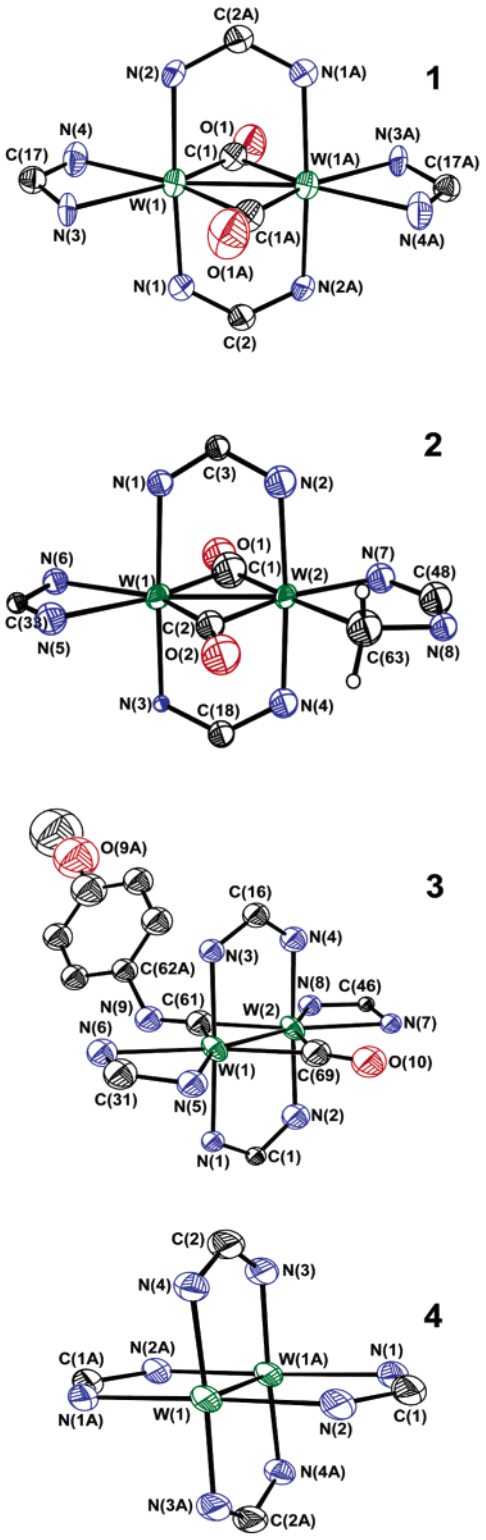

Figure 1. Thermal ellipsoid plots at the 50% probability level for $W_2(\mu\text{-}CO)_2(\mu\text{-}DAniF)_2(\eta^2\text{-}DAniF)_2$ (**1**), $W_2(\mu\text{-}CO)_2(\mu\text{-}DAniF)_2(\eta^2\text{-}DAniF)(\eta^2\text{-}CH_2DAniF)$ (**2**), $W_2(\mu\text{-}CO)(\mu\text{-}CNC_6H_4OCH_3)(\mu\text{-}DAniF)_2(\eta^2\text{-}DAniF)_2$ (**3**), and $W_2(DAniF)_4$ (**4**). H atoms and the aryl groups on the formamidinate ligands are removed for clarity.

(23) (a) Carlson-Day, K. M.; Eglin, J. L.; Smith, L. T.; Staples, R. J. *Inorg. Chem.* **1999**, *38*, 2216. (b) Eglin, J. L.; Smith, L. T.; Staples, R. J. *Inorg. Chim. Acta* **2003**, *351*, 217.

Table 2. Bond Parameters (Å or deg) for **1**

W(1)−W(1A)	2.476(1)	W(1)−C(1)−O(1)	163(1)
W(1)−N(1)	2.137(9)	W(1A)−C(1)−O(1)	126.2(9)
W(1)−N(2)	2.103(9)	W(1)−C(1)−W(1A)	70.6(4)
W(1)−N(3)	2.202(8)	C(1)−W(1)−W(1A)	60.2(3)
W(1)−N(4)	2.211(9)	C(1)−W(1A)−W(1)	49.2(3)
W(1)−C(1)	1.99(1)	N(1)−W(1)−N(2)	176.5(3)
W(1)−C(1A)	2.28(1)	N(3)−W(1)−N(4)	59.9(4)
C(1)−O(1)	1.16(1)	N(1)−W(1)−N(3)	91.0(3)
N(1)−C(2)	1.32(1)	N(1)−W(1)−N(4)	95.1(4)

is large. Other ditungsten edge-sharing bioctahedra, such as W$_2$(D^{Cl}PhF)$_4$(μ-OH)$_2$[23a] and W$_2$(DTolF)$_4$(μ-OH)$_2$,[24] have core structures that are essentially symmetrical, which intuitively suggests that these π-accepting CO ligands are directly involved in the orbital interactions that favor this distortion. Furthermore, the W(1)−C(1)−O(1) bond angle of 163(1)° in **1** approaches the linearity that would be expected for a terminal rather than a bridging CO ligand, while the C(1)−W(1)−W(1A) bond angle is 60.2(3)°. Using the structural criteria described by Crabtree and Lavin,[25] **1** meets the definition of a type II linear semibridging carbonyl system.

Identification of the CH$_2$DAniF ligand in **2** rests upon the collective evidence of ^{1}H and ^{13}C NMR spectroscopy in addition to mass spectroscopy, X-ray crystallography, and elemental analysis. The −C*H*$_2$− resonance occurs as a broadened singlet at 3.10 ppm in the ^{1}H NMR spectrum of **2** with an integrated intensity corresponding to two hydrogen atoms. The methylenic carbon nucleus is observed at 69.40 ppm in the ^{13}C NMR spectrum, a value similar to that of 68.40 ppm reported for the closely related compound W$_2$(μ-CO)$_2$(μ-D^{3,5}XylF)$_2$(η-D^{3,5}XylF)(η-CH$_2$D^{3,5}XylF).[26] The ESI$^+$ mass spectrum of **2** displays a parent ion peak with an isotope distribution profile matching the formulation given for this compound. Refinement of the X-ray diffraction data for **2** produces a more reasonably sized thermal ellipsoid for the atom in question when it is identified as carbon rather than as a heteroatom such as nitrogen or oxygen. Furthermore, the analytical data are consistent with the presence of an additional methylene group.

The core structures of **2** and **3** are set forth in Figure 1, and Tables 3 and 4 summarize relevant bond parameters. In all essential respects, these three compounds are very similar with W−W bond lengths in the narrow range 2.473(1)−2.4803(9) Å. As with **1**, both of these compounds have a skewed W$_2$(μ-X)$_2$ core structure, although the symmetry lowering is somewhat less exaggerated. Replacement of the DAniF ligand by CH$_2$DAniF in **2** and of μ-CO by μ-CNC$_6$H$_4$OCH$_3$ in **3** produces little effect on the other structural parameters of these compounds. The C(61)−N(9)−C(62A) bond angle of 129(2)° observed for the bridging isonitrile ligand in **3** is characteristic for this ligand type in this coordination mode.[27]

Table 3. Bond Parameters (Å or deg) for **2**

W(1)−W(2)	2.4803(9)	W(1)−C(1)−O(1)	130(2)
W(1)−C(1)	2.15(3)	W(2)−C(1)−O(1)	156(2)
W(2)−C(1)	1.99(3)	W(1)−C(2)−O(2)	158(2)
C(1)−O(1)	1.20(3)	W(2)−C(2)−O(2)	129(2)
W(1)−C(2)	2.02(2)	C(1)−W(1)−W(2)	50.3(8)
W(2)−C(2)	2.25(2)	C(1)−W(2)−W(1)	56.2(8)
C(2)−O(2)	1.14(4)	N(5)−W(1)−N(6)	56.9(6)
W(2)−C(63)	2.21(2)	W(2)−C(63)−N(8)	110(1)
N(8)−C(63)	1.58(2)	N(7)−W(2)−C(63)	78.7(7)

Table 4. Bond Parameters (Å or deg) for **3**

W(1)−W(2)	2.473(1)	W(1)−C(69)−W(2)	72(1)
W(1)−C(69)	1.99(3)	W(1)−C(61)−W(2)	72.4(9)
W(2)−C(69)	2.21(3)	W(1)−C(69)−O(10)	156(2)
W(1)−C(61)	2.21(3)	W(2)−C(69)−O(10)	133(2)
W(2)−C(61)	1.96(3)	W(1)−C(61)−N(9)	129(2)
C(69)−O(10)	1.15(3)	W(2)−C(61)−N(9)	158(2)
C(61)−N(9)	1.27(4)	C(69)−W(1)−W(2)	58.1(6)
W(1)−N(1)	2.15(2)	C(69)−W(2)−W(1)	50.0(7)
W(1)−N(3)	2.14(2)	C(61)−N(9)−C(62A)	129(2)

Collectively, **1**−**3** account for ∼20% of the tungsten starting material. The observation of persistent CO in these products indicates that W(CO)$_6$ is intrinsically less reactive and undergoes loss of CO less readily than Cr(CO)$_6$ and Mo(CO)$_6$. The forcing conditions that are required to initiate any reaction with HDAniF approach the limits of the thermal stability of this type of ligand. It is difficult to "explain" unambiguously how the η-CH$_2$DAniF ligand in **2** and the μ-C═N−C$_6$H$_4$OCH$_3$ ligand in **3** form. However, there are precedents for considerable reactivity of formamidines, and numerous products bearing modified forms of this kind of ligand have been isolated and characterized.[28] It is possible that N−C bond scission could produce a transient isonitrilium species that could either proceed to form the μ-CNC$_6$H$_4$OCH$_3$ molecule (**3**) or undergo some form of self-coupling that ultimately leads to the CH$_2$DAniF ligand in **2**. Alternatively, CH$_2$DAniF may result from CO insertion into a W−N bond with subsequent reduction by excess HDAniF, as has been suggested for the isostructural compound W$_2$(D^{3,5}XylF)$_3$(CH$_2$D^{3,5}Xyl)(μ-CO)$_2$.[26] Thus, it is likely that the success in preparing W$_2$(mhp)$_4$ (mhp = the deprotonated form of 2-hydroxy-6-methylpyridine)[6a] and W$_2$(dmhp)$_4$ (dmhp = the deprotonated form of 2,4-dimethyl-2-hydroxypyrimidine)[6c] directly from W(CO)$_6$ owes much to the stability of these ligands under the forcing conditions that are required.

The quadruply bonded tetragonal paddlewheel compound, **4**, while not accessible from W(CO)$_6$, may be prepared in moderate yields from WCl$_4$/KC$_8$. Its color is red-orange in the crystalline state, and its structural parameters (Table 5) closely coincide with values observed in other crystallographically characterized ditungsten tetraformamidinate complexes.[23,29] The analogous compound W$_2$(D^{Cl}PhF)$_4$ (D^{Cl}PhF = *N*,*N*′-di-(3,5-dichlorophenyl)formamidinate) may be prepared by a similar method.[30] When recrystallized from the reaction mixture without rigorous exclusion of air and moisture, W$_2$(D^{Cl}PhF)$_4$ is susceptible to a slow transformation

(24) Cotton, F. A.; Daniels, L. M.; Ren, T. *Inorg. Chem.* **1999**, *38*, 2221.
(25) Crabtree, R. H.; Lavin, M. *Inorg. Chem.* **1986**, *25*, 805.
(26) (a) Schagen, J. D.; Schenk, H. *Cryst. Struct. Commun.* **1978**, *7*, 223. (b) de Roode, W. H.; Vrieze, K. *J. Organomet. Chem.* **1978**, *145*, 207.
(27) (a) Yamamoto, Y. *Coord. Chem. Rev.* **1980**, *32*, 193. (b) Chisholm, M. H.; Clark, D. L.; Ho, D.; Huffman, J. C. *Organometallics* **1987**, *6*, 1532.
(28) See for example: Cotton, F. A.; Daniels, L. M.; Matonic, J. H.; Wang, X.; Murillo, C. A. *Polyhedron* **1997**, *16*, 1177 and references therein.
(29) Cotton, F. A.; Ren, T. *J. Am. Chem. Soc.* **1992**, *114*, 2237.

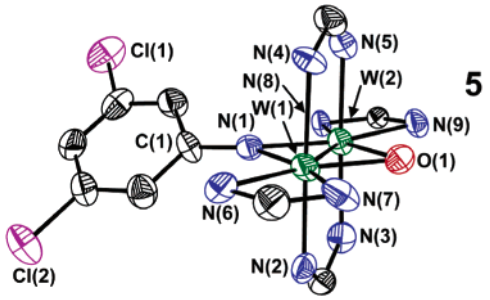

Figure 2. Thermal ellipsoid plot at the 50% probability level for $W_2(\mu\text{-O})(\mu\text{-NC}_6H_3Cl_2)(\mu\text{-D}^{Cl}PhF)_2(\eta^2\text{-D}^{Cl}PhF)_2$ (**5**). H atoms and the aryl groups on **5** are omitted for clarity.

Table 5. Bond Parameters (Å or deg) for **4**

W(1)−W(1A)	2.1956(5)	N(1A)−W(1)−N(2)	176.50(9)
W(1)−N(2)	2.131(3)	N(3A)−W(1)−N(4)	176.59(8)
W(1)−N(4)	2.135(3)	N(1A)−W(1)−N(3A)	88.9(1)
W(1)−N(1A)	2.131(3)	N(1A)−W(1)−N(4)	90.0(1)
W(1)−N(3A)	2.126(3)	N(2)−W(1)−N(3A)	89.9(1)
N(1)−C(1)	1.335(4)	N(2)−W(1)−N(4)	91.1(1)
N(2)−C(1)	1.336(4)	N(2)−W(1)−W(1A)	90.49(7)
N(3)−C(2)	1.331(4)	N(1)−C(1)−N(2)	120.5(3)
N(4)−C(2)	1.333(4)	N(3)−C(2)−N(4)	120.8(3)

Table 6. Bond Parameters (Å or deg) for **5**

W(1)−W(2)	2.3972(9)	W(1)−N(1)−W(2)	74.5(3)
W(1)−N(1)	1.993(9)	W(1)−O(1)−W(2)	75.4(3)
W(2)−N(1)	1.968(9)	N(1)−W(1)−O(1)	104.7(3)
W(1)−O(1)	1.956(8)	N(1)−W(2)−O(1)	105.4(3)
W(2)−O(1)	1.964(7)	O(1)−W(1)−W(2)	52.5(2)
W(1)−N(6)	2.193(9)	O(1)−W(2)−W(1)	52.1(2)
W(1)−N(7)	2.170(9)	N(1)−W(1)−W(2)	52.3(3)
W(2)−N(8)	2.205(8)	W(1)−N(1)−C(1)	146.4(8)
W(2)−N(9)	2.188(9)	W(2)−N(1)−C(1)	138.5(7)

to $W_2(\mu\text{-O})(\mu\text{-NC}_6H_3Cl_2)(\mu\text{-D}^{Cl}PhF)_2(\eta^2\text{-D}^{Cl}PhF)_2$ (**5**), which crystallizes in the form of thin green plates. The core structure of **5**, which is a ditungsten(IV,IV) compound, is presented in Figure 2. Identification of the bridging ligand as oxo rather than hydroxo is based in part upon the diamagnetism of the compound, which requires the oxygen ligand to be isoelectronic to the imido ligand so as to provide an even charge to the ditungsten core. The metal−metal bond distance in **5** (2.3972(9) Å, Table 6) is slightly shorter than those observed in **1**−**3** even though the metal−metal bond order is probably two as well (vide infra). We note, however, that **5** would have tungsten−tungsten double bond with a $\sigma^2\pi^2$ configuration while compounds **1**−**3** would have a $\sigma^2\pi^2\sigma^{*2}\delta^2$ electron configuration. Although the nature of the tungsten−tungsten double bond in **5** differs from that in these other compounds, the metal−metal distance is still within the range that would expected for a bond order of two. Once formed, **5** is quite stable to air. Small quantities of bright yellow *N*-(3,5-dichlorophenyl)formamide[31] could also be isolated from the same crystallization flask that yielded **5**. The observation of *N*-(3,5-dichlorophenyl)formamide, which by ^{1}H NMR spectroscopy is not an impurity in the $HD^{Cl}PhF$ starting material, suggests that the μ-N−$C_6H_3Cl_2$ ligand in **5** originates from free aniline that is produced from hydrolysis of trace $HD^{Cl}PhF$ by adventitious water:

$$(3,5\text{-}Cl_2C_6H_3)NHC(H){=}N(3,5\text{-}Cl_2C_6H_3) + H_2O \rightarrow H_2N{-}(3,5\text{-}Cl_2C_6H_3) + (3,5\text{-}Cl_2C_6H_3)N(H)CHO \quad (1)$$

Electrochemistry. Cyclic voltammetry upon **1** in CH_2Cl_2 (Figure 3) reveals two successive one-electron oxidations at 0.510 and 0.991 V relative to Ag/AgCl. The relatively mild potential at which the first oxidation occurs suggests that it may be feasible to chemically prepare and isolate the $[W_2(\mu\text{-CO})_2(\mu\text{-DAniF})_2(\eta^2\text{-DAniF})_2]^+$ cation with a suitable counterion. Both oxidations appear to be reversible as judged by the relatively loose criterion that they display symmetric peak current on the forward and reverse scans without diminution over repeated cycles. Compounds **2** and **3** are more readily oxidized than **1**, and the potentials are 0.373 and 0.207 V, respectively. For **2**, this is probably because the CH_2DAniF ligand is somewhat more electron rich than the unmodified formamidinate while in **3** this reflects the better π-accepting ability of a carbonyl over an isonitrile ligand. Surprisingly, **2** has no other features within the potentials accessible in CH_2Cl_2, but **3** does have a quasi-reversible wave at 0.763 V (scan rate of 100 mV/s). At scan rates ≥200 mV/s, this wave appears reversible.

The compound $W_2(DAniF)_4$ displays a reversible wave at −0.336 V in its cyclic voltammogram (Figure 3), which is assigned as a one-electron oxidation of the W_2^{4+} core to W_2^{5+}. Compared to its dimolybdenum homologue (Figure 3),[32] $W_2(DAniF)_4$ is more easily oxidized by 0.486 V, which is consistent with the general observation that, at parity of ligand, tungsten complexes are more readily oxidized than their molybdenum counterparts.[33] The only other ditungsten tetraformamidinate complex to have been examined by electrochemistry is $W_2(DTolF)_4$[29] (DTolF = *N*,*N*′-di-*p*-tolylformamidinate), which undergoes a reversible one-electron oxidation at +0.070 V when adjusted to the Ag/AgCl reference that we have used. This number is consistent with the significantly greater electron donating character of the DAniF ligand compared to DTolF.

DFT Calculations and Electronic Structures. Compounds **1**−**3** and **5** are edge-sharing bioctahedra, a common structure type for which detailed analyses of the electronic structure have been given.[34] In most instances, these edge-sharing bioctahedra have symmetric core structures in contrast to the pronounced distortion from D_{2h} to C_{2h} symmetry observed in **1**−**3**. To obtain more insight into the basis for the skewed $W_2(\mu\text{-CO})_2$ core structures in this set of compounds, DFT calculations were undertaken on two

(30) The reported crystal structure for $W_2(D^{Cl}PhF)_4$ is of the tetrakis(THF) solvate. See ref 23. We obtained crystalline samples of $W_2(D^{Cl}PhF)_4$ from CH_2Cl_2 without interstitial solvent: space group = $P\bar{1}$, a = 9.823(1) Å, b = 11.715(1) Å, c = 14.377(2) Å, α = 97.897(2)°, β = 104.285(2)°, γ = 113.530(2)°, V = 1417.2(3) Å^3, Z = 1, R1 = 0.039, wR2 = 0.080. Additional crystallographic data are provided as Supporting Information.

(31) Crystallographic data for *N*-(3,5-dichlorophenyl)formamide are as follows: space group = *Cc*, a = 7.943(1) Å, b = 14.724(2) Å, c = 7.292(1) Å, β = 109.526(2)°, V = 803.7(2) Å^3, Z = 4, R1 = 0.043, wR2 = 0.117. Additional crystallographic data are provided as Supporting Information.

(32) Cotton, F. A.; Donahue, J. P.; Murillo, C. A. *J. Am. Chem. Soc.* **2003**, *125*, 5436.
(33) Tucci, G. C.; Donahue, J. P.; Holm, R. H. *Inorg. Chem.* **1998**, *37*, 1602.
(34) Cotton, F. A. *Polyhedron* **1987**, *6*, 667.

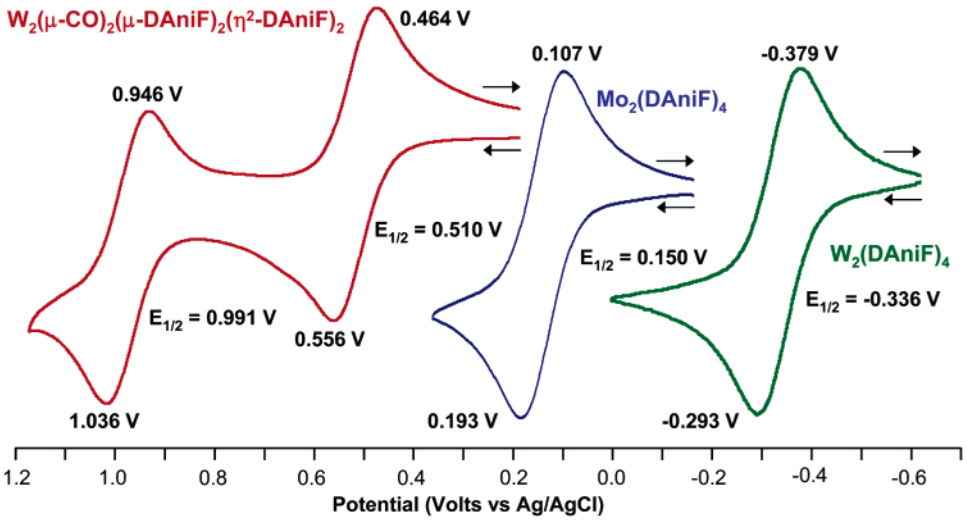

Figure 3. Cyclic voltammograms in CH_2Cl_2 of $W_2(\mu\text{-}CO)_2(\mu\text{-}DAniF)_2(\eta^2\text{-}DAniF)_2$ (in red), $Mo_2(DAniF)_4$ (in blue), and $W_2(DAniF)_4$ (in green). The electrochemical data for $Mo_2(DAniF)_4$ was initially presented in ref 32.

Table 7. Results of the DFT Calculations upon $W_2(\mu\text{-}CO)_2(\mu\text{-}DAniF)_2(\eta^2\text{-}DAniF)_2$

		bond length, Å			
model	energy (au)	W−W	C═O	W(1)−CO	W(2)−CO
D_{2h}	−960.0696	2.4560	1.2187	2.1093	2.1093
C_{2h}	−960.0776	2.4898	1.2194	2.3367	1.9665
exptl		2.476(1)	1.16(1)	2.28(1)	1.99(1)

models of **1**. An additional objective was to determine a plausible description of the bond order between the tungsten atoms in **1**.

The DFT calculations were expedited by substituting the *p*-anisyl groups in **1** with hydrogen atoms, a simplification that has previously yielded satisfactory results on similar systems.[35] The geometries of two models for **1** were optimized by constraining them to conform to D_{2h} symmetry in one case and to C_{2h} symmetry in the other. Some results of these DFT calculations are presented in Table 7. The calculated tungsten−tungsten distance in the D_{2h} model is appreciably shorter than that found in the crystal structure, while the value obtained for the C_{2h} model is slightly longer and in better agreement with the measured distance (a difference of ∼0.01 Å). In both the D_{2h} and C_{2h} models, the carbon−oxygen bond length of the bridging carbonyl ligands increases significantly over that of free C≡O, an effect that is attributed to back-bonding from the tungsten atoms into the ligand π^* orbitals. Finally, the W−CO distances in the C_{2h} model are calculated to be 2.34 and 1.97 Å, which indicates one strong and one weak interaction with the metal atoms, while the value of 2.11 Å for the D_{2h} system reflects two intermediate, symmetrical W−CO interactions.

The DFT calculations reveal that the C_{2h} model is 0.22 eV (5.08 kcal/mol) lower in energy than the D_{2h} model. The structure with D_{2h} symmetry represents a transition state for interconversion between the two C_{2h} structures, as implied by an imaginary frequency at 366i cm^{-1}. This transition state is readily accessible at room temperature in solution, as indicated by the ^{1}H NMR spectrum of **1**, which shows two symmetric DAniF ligands in a 1:1 ratio, both halves of each type of the DAniF ligand being the same. Similar dynamic solution behavior for semilinear bridging carbonyl ligands has been observed by ^{1}H NMR in other ditungsten systems.[36]

The electronic structures of the D_{2h} and C_{2h} models differ from each other principally in the degree of overlap between the CO ligands and the metal orbitals. The ordering of the frontier molecular orbitals resembles the electronic configuration previously established for edge-sharing bioctahedra[34] but with some differences. Figure 4 illustrates the DFT-calculated frontier molecular orbitals for the C_{2h} symmetric model for **1**. The HOMO − 3 (a_g) and the HOMO − 2 (a_u) are clearly metal-based σ and π type MOs, respectively. The HOMO − 1 (b_u) is primarily metal-based also but is σ^* in character since it is composed of the out-of-phase combination of the two $d_{x^2-y^2}$ orbitals. In conventional edge-sharing bioctahedra,[34] this MO is expected to be high in energy, but in **1** it is greatly stabilized by a back-bonding interaction with one of the π^* orbitals of the μ-CO ligands, as can be seen in Figure 4. The HOMO (b_g), which shows a bonding tungsten−tungsten interaction of δ symmetry, reveals back-bonding into the second set of π^* orbitals of the μ-CO ligands. These interpretations of the DFT results are consistent with the IR stretching frequency of 1747 cm^{-1} observed for the μ-CO ligands in **1**, which is toward the lower energy end of the 1700−1860 cm^{-1} range[37] in which bridging CO ligands in neutral molecules absorb and thus indicates strong metal-to-ligand back-bonding. Our formulation of the $W_2(\mu\text{-}CO)_2$ system in **1** as a π donor−π acceptor interaction between the tungsten−tungsten multiple bond and the μ-CO ligands is a description that qualitatively agrees with the bonding analysis in other types of dimetal systems with linear semibridging carbonyl ligands.[38]

(35) (a) Cotton, F. A.; Donahue, J. P.; Murillo, C. A.; Pérez, L. M. *J. Am. Chem. Soc.* **2003**, *125*, 5486. (b) Cotton, F. A.; Donahue, J. P.; Murillo, C. A.; Pérez, L. M.; Yu, R. *J. Am. Chem. Soc.* **2003**, *125*, 8900.

(36) (a) Carriedo, G. A.; Howard, J. A. K.; Jeffery, J. C.; Sneller, K.; Stone, F. G. A.; Weerasuria, A. M. M. *J. Chem. Soc., Dalton Trans.* **1990**, 953. (b) Alvarez, M. A.; García, M. E.; Riera, V.; Ruiz, M. A.; Falvello, L. R.; Bois, C. *Organometallics* **1997**, *16*, 354.

(37) Cotton, F. A.; Wilkinson, G. *Advanced Inorganic Chemistry*; Wiley: New York, 1988; p 1034.

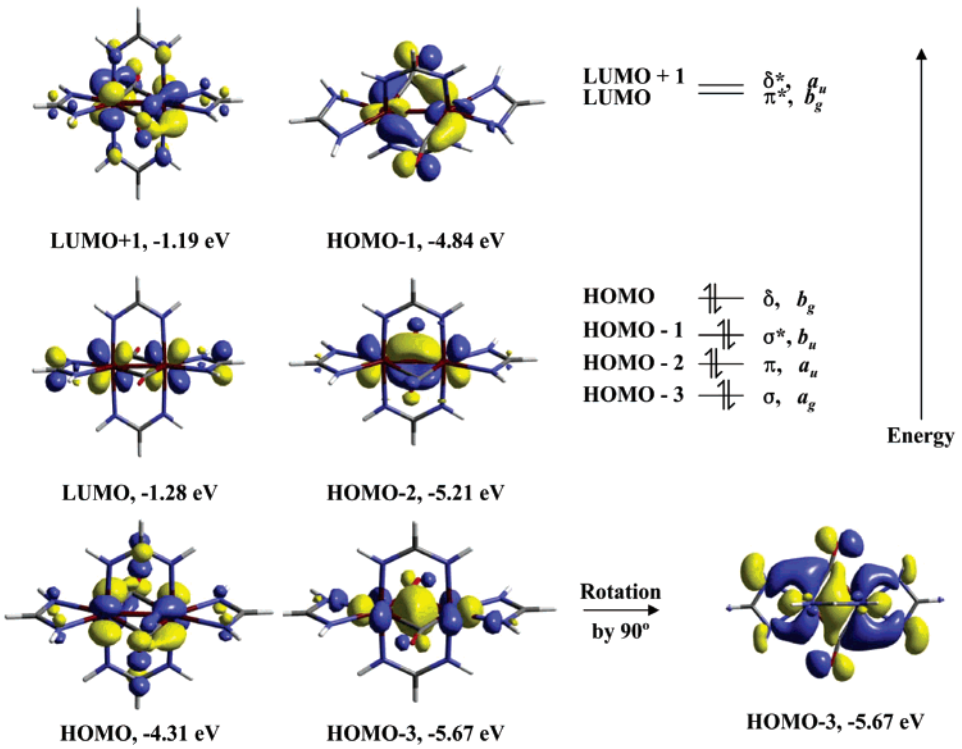

Figure 4. Illustration of the 0.04 contour surface diagrams for the DFT calculated four highest occupied and two lowest unoccupied MOs for the model of $W_2(\mu\text{-CO})_2(\mu\text{-DAniF})_2(\eta^2\text{-DAniF})_2$ with C_{2h} symmetry. The alternate view of the HOMO − 3 is presented with a 0.05 contour surface. The *z* axis is taken to be perpendicular to the plane defined by the tungsten atoms and μ-CO ligands.

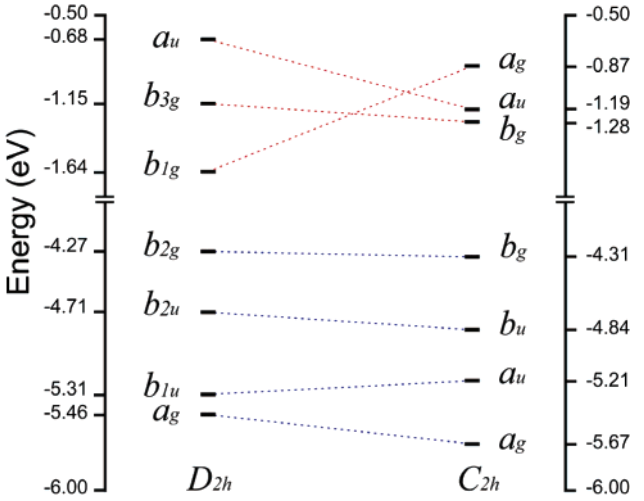

Figure 5. Orbital correlation diagram for **1** illustrating the changes in energy of the four highest occupied (dashed blue lines) and three lowest unoccupied (dashed red lines) MOs in moving from D_{2h} to C_{2h} symmetry.

The basis for the D_{2h} to C_{2h} distortion in **1** is most clearly revealed by the orbital correlation diagram in Figure 5. In going from D_{2h} to C_{2h} by skewing of the CO ligand bridges, the HOMO − 3 (a_g) σ type orbital is stabilized appreciably (0.21 eV). This increased stabilization is due to the better overlap, and consequently better back-bonding interaction, of the μ-CO π^* orbitals with the tungsten $d_{x^2-y^2}$ orbitals that constitute the σ bond, a point which is readily seen by the alternate presentation of the HOMO − 3 in Figure 4. In the D_{2h} geometry, the CO π^* orbitals interact in nonbonding fashion with this σ bond. The D_{2h} to C_{2h} distortion has a lesser effect on the π (HOMO − 2, b_{1u}) and σ^* (HOMO − 1, b_{2u}) orbitals, respectively destabilizing and stabilizing them by similar amounts (~0.1 eV). The increase in energy of the HOMO − 2 is apparently due to a slight movement of the tungsten d_{yz} orbitals out of their plane of interaction, which lowers their direct overlap. The energy of the δ orbital (HOMO, b_{2g}) is only slightly lowered by the D_{2h} to C_{2h} symmetry change despite the fact that it is also an orbital with appreciable tungsten-to-CO π^* back-bonding character.

Some dimolybdenum(IV,IV) edge-sharing bioctahedra with two μ-oxo ligands show slight skewing of the $Mo_2(\mu\text{-}O)_2$ core (average Mo−O bond lengths are 1.911(1) and 1.965(1) Å), and this was attributed to a second-order Jahn−Teller effect involving the HOMO and LUMO.[39] This same effect is not operative in **1** because the b_{1g} vibration which involves the μ-CO ligands in the D_{2h} point group does not couple the HOMO (b_{2g}) and LUMO (b_{1g}) (i.e., $b_{2g} \otimes b_{1g} \otimes b_{1g} \neq a_g$). However, the b_{1g} vibration does couple the HOMO − 3 with the LUMO. While the difference in energy between these two orbitals is appreciable (3.82 eV), it appears that such coupling may contribute to the stabilization of the HOMO − 3 and hence the distortion from D_{2h} to C_{2h} symmetry.

The ordering of the frontier MOs as presented in Figure 4 provides a clear basis for formulating the tungsten−tungsten bond order as two. The HOMO − 3 and HOMO − 2 are principally tungsten based and are bonding in nature (σ and

(38) (a) Morris-Sherwood, B. J.; Powell, C. B.; Hall, M. B. *J. Am. Chem. Soc.* **1984**, *106*, 5079. (b) Sargent, A. L.; Hall, M. B. *J. Am. Chem. Soc.* **1989**, *111*, 1563. (c) Sargent, A. L.; Hall, M. B. *Polyhedron* **1990**, *9*, 1799.

(39) Cotton, F. A.; Daniels, L. M.; Murillo, C. A.; Slaton, J. G. *J. Am. Chem. Soc.* **2002**, *124*, 2878.

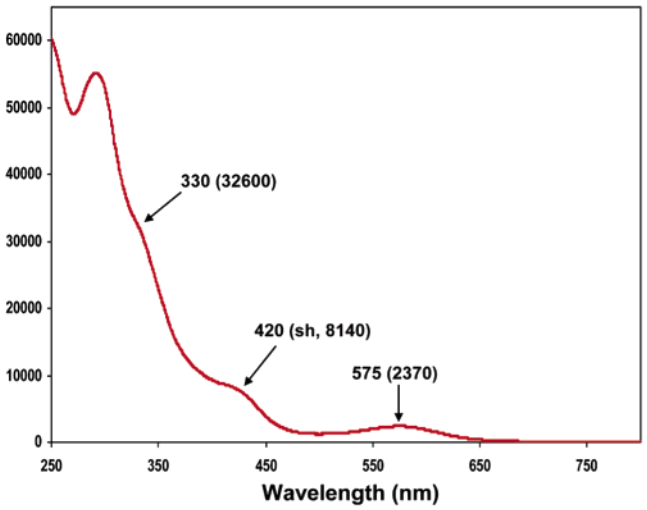

Figure 6. Electronic absorption spectrum in CH_2Cl_2 for $W_2(\mu\text{-CO})_2(\mu\text{-DAniF})_2(\eta^2\text{-DAniF})_2$.

π, respectively). The HOMO − 1 and the HOMO are constituted in large part from the tungsten atoms although they also have appreciable character from the μ-CO π^* orbitals. While the HOMO − 1 is antibonding (σ^*) with respect to the tungsten−tungsten interaction, the HOMO is bonding (cf. Figure 4), and the two effectively cancel one another to leave a net bond order of two between the metal atoms. The W(1)−W(1A) bond length of 2.476(1) Å in **1** corresponds well to a double bond as it is intermediate in length between the metal−metal bond distances in well characterized singly[40] and triply[41] bonded ditungsten compounds and consistent with other ditungsten doubly bonded compounds.[42]

A time-dependent DFT calculation on the geometry optimized C_{2h} compound was performed to ascertain the nature of the lowest energy transition in **1** (Figure 6). The calculations indicate that this absorption is due to a HOMO → LUMO + 1 transition that is essentially $\delta \rightarrow \delta^*$ in character. The calculated transition energy (oscillator strength $f = 0.0036$) at 538 nm agrees reasonably well with the observed excitation at 575 nm ($\epsilon = 2370$). The energy of this transition is somewhat lower than the pure $\delta \rightarrow \delta^*$ transitions observed in typical quadruply bonded paddlewheel complexes (e.g., 412, sh) for **4** and reflects the longer tungsten−tungsten distance and lowered bond order.

(40) See for example: (a) Chisholm, M. H.; Cotton, F. A.; Extine, M. W.; Murillo, C. A. *Inorg. Chem.* **1978**, *17*, 696. (b) Bino, A.; Cotton, F. A.; Dori, Z.; Sekutowski, J. C. *Inorg. Chem.* **1978**, *17*, 2946.

(41) See for example: (a) Chisholm, M. H.; Cotton, F. A.; Extine, M.; Stults, B. R. *J. Am. Chem. Soc.* **1976**, *98*, 4477. (b) Chisholm, M. H.; Cotton, F. A.; Extine, M.; Millar, M.; Stults, B. R. *Inorg. Chem.* **1976**, *15*, 2244. (c) Chisholm, M. H.; Cotton, F. A.; Extine, M.; Stults, B. R. *Inorg. Chem.* **1976**, *15*, 2252. (d) Blatchford, T. P.; Chisholm, M. H.; Huffman, J. C. *Inorg. Chem.* **1987**, *26*, 1920. (e) Chisholm, M. H.; Clark, D. L.; Folting, K.; Huffman, J. C.; Hampden-Smith, M. *J. Am. Chem. Soc.* **1987**, *109*, 7750.

(42) See for example: (a) Anderson, L. B.; Cotton, F. A.; DeMarco, D.; Fang, A.; Ilsley, W. H.; Kolthammer, B. W. S.; Walton, R. A. *J. Am. Chem. Soc.* **1981**, *103*, 5078. (b) Cotton, F. A.; Falvello, L. R.; Fredrich, M. F.; DeMarco, D.; Walton, R. A. *J. Am. Chem. Soc.* **1983**, *105*, 3088.

Scheme 3. The Molecule from Which the hpp Ligand Is Derived

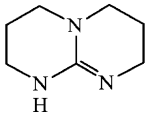

Summary and Conclusions

Tungsten carbonyl, $W(CO)_6$, is much less reactive toward HDAniF than its molybdenum and chromium analogues; CO tends to remain bound to the tungsten atoms even under conditions that cause decomposition of the formamidine. Several ditungsten carbonyl species, the most interesting of which is $W_2(\mu\text{-CO})_2(\mu\text{-DAniF})_2(\eta^2\text{-DAniF})_2$ (**1**), have been isolated. This compound is produced in low yield mixed with related compounds (**2** and **3**). Compounds **2** and **3** reveal degradation of the HDAniF ligand under the harsh reaction conditions that are necessary to induce reaction with $W(CO)_6$. Preparation of the tetragonal paddlewheel $W_2(DAniF)_4$ (**4**) does not appear to be feasible starting from $W(CO)_6$, but it is accessible from WCl_4 by established procedures. Solutions of $W_2(D^{Cl}PhF)_4$, prepared by the same method as for **4**, undergo decomposition upon exposure to air to the novel oxo-imido compound $W_2(\mu\text{-O})(\mu\text{-NC}_6H_3Cl_2)(\mu\text{-D}^{Cl}PhF)_2(\eta^2\text{-D}^{Cl}PhF)_2$ (**5**), in which the imido ligand appears to have originated from hydrolysis of $HD^{Cl}PhF$ to 3,5-dichloroaniline and *N*-(3,5-dichlorophenyl)formamide (eq 1).

Calculations at the DFT level on **1** reveal that its C_{2h} geometry is energetically favored over a more symmetric D_{2h} structure because of strong W → CO π^* back-bonding. Both orthogonal CO π^* orbitals are engaged as π acceptors. The system favors a strong−weak pair of W−CO interactions over the symmetric pair of W−CO bond distances because the resulting skewed $W_2(\mu\text{-CO})_2$ core structure permits each μ-CO ligand to approach linearity with one W atom and results in greatly enhanced metal-to-ligand back-bonding. Constraining the molecular geometry to D_{2h} symmetry diminishes this metal-to-ligand back-bonding but produces an appreciable shortening of the tungsten−tungsten bond distance, indicating that the former interaction occurs largely at the expense of the latter. The tungsten−tungsten bond is an unambiguous double bond, and the lowest energy absorption of **1** at 575 nm is a HOMO → LUMO + 1 excitation that is best described as being a $\delta \rightarrow \delta^*$ transition. The skewed $W_2(\mu\text{-CO})_2/W_2(\mu\text{-CO})(\mu\text{-CNC}_6H_4OCH_3)$ core structures in **2** and **3** undoubtedly have fundamentally the same origin as that found for **1**.

While our results make it clear that a direct synthetic route to ditungsten tetragonal paddlewheel compounds from $W(CO)_6$ is not feasible with formamidine ligands because of their susceptibility to decomposition, this limitation does not necessarily extend to other anionic nitrogen bridging ligands that have been used to support dimetal units. In particular, the hpp ligand (hpp = the anion of 1,3,4,6,7,8-hexahydro-2*H*-pyrimido[1,2-*a*]pyrimidine, Scheme 3), which has been extensively studied in this laboratory and elsewhere, has consistently proven to be a more robust ligand that is capable of stabilizing oxidation states in dimetal units that cannot be accessed by the analogous formamidinate com-

plexes. One of the felicitous features of the hpp ligand is the resistance toward C−N scission degradation within the guanidinate core because of the protection afforded by the exocyclic six membered rings.[43] Continuing research in this laboratory will include a similar careful examination of the reaction of $W(CO)_6$ with Hhpp, which we anticipate will reveal marked differences with the formamidinate system.

Acknowledgment. We thank the National Science Foundation and the Robert A. Welch Foundation for funding the research reported here. Helpful discussions with Dr. Steve Silber regarding the ^{1}H NMR spectra of the compounds reported here and with Dr. Xiaoping Wang concerning aspects of the crystallographic characterization of these compounds are very much appreciated. J.P.D. acknowledges the support of an NIH postdoctoral fellowship.

Supporting Information Available: Thermal ellipsoid plots at the 50% probability level with complete atomic labeling in PDF format in addition to X-ray crystallographic data for compounds **1**−**5** in standard CIF format. Crystallographic information for the structures cited in refs 30 and 31 as well as molecular orbitals of the D_{2h} model of $W_2(\mu\text{-CO})_2(\mu\text{-DAniF})_2(\eta^2\text{-DAniF})_2$. This material is available free of charge via the Internet at http://pubs.acs.org.

IC049116C

(43) Cotton, F. A.; Matonic, J. H.; Murillo, C. A. *J. Am. Chem. Soc.* **1998**, *120*, 6047.